DOMAIN DECOMPOSITION METHODS FOR SENSITIVITY ANALYSIS OF A NONLINEAR AEROELASTICITY PROBLEM*

OMAR GHATTAS† AND XIAOGANG LI‡

Abstract. We consider the nonlinear aeroelasticity problem of the interaction between a viscous, incompressible fluid and an elastic solid undergoing large displacement. The nonlinearities of the problem formulation include the solid and fluid governing equations, as well as the dependence of the flow geometry on the solid deformation. The resulting coupling is thus two-way. We develop domain-decomposition methods for solution and sensitivity analysis of the coupled problem. The domain decomposition is in the form of a block-Gauss-Seidel-like preconditioner that decomposes the coupled-domain problem into distinct nonoverlapping fluid and solid subdomain problems. The preconditioner thus enables exploitation of single-domain algorithms for solid and fluid mechanics discretization and solution. On the other hand, two-way fluid-solid coupling is retained within the residuals, which is essential for correct sensitivities. Sensitivities of field quantities can be found with little additional work beyond that required for solving the coupled fluid-solid system. The methodology developed here is illustrated by the solution of a problem of viscous incompressible flow about an infinite elastic cylinder. Sensitivities of the resulting velocity and displacement fields with respect to elastic modulus and fluid viscosity are computed.

Key words. Sensitivity analysis, nonlinear aeroelasticity, fluid-solid interaction, Navier-Stokes flows, finite elasticity, domain decomposition methods, finite element methods, variational methods.

1. Introduction. Sensitivity analysis of a physical system is the computation of derivatives of its state variables with respect to parameters upon which the response of the system explicitly and implicitly depends. State variable sensitivities are an essential ingredient in efficient algorithms for optimal design. This stems from the fact that optimality is characterized by the vanishing of the gradient (with respect to design parameters) of the objective function of a design problem within a subspace orthogonal to the Jacobian (with respect to design parameters) of its constraints. For objectives and constraints that are functions of state variables, then, the crucial step is finding derivatives of these variables with respect to the design parameters.

A central challenge in multidisciplinary design optimization is the development of methods for sensitivity analysis of coupled multidomain problems. Prominent among these problems is that of the nonlinear interaction of fluid and solid. When the solid undergoes large displacement, the system is tightly coupled in both directions: deformation of the solid changes the flow physics, which change the tractions induced on the solid, which further deform the solid, etc. When the fluid is air, this problem is known as the nonlinear aeroelasticity problem. Here, we consider a nonlinear aeroelasticity problem of the steady interaction between a viscous, incompressible fluid, and an elastic solid undergoing large displacement. In addition to nonlinearities present in both fluid and solid behavior, we account for the dependence of the flow domain on the deforming interface. Such models find application to design problems of flexible structures under aerodynamic or hydrodynamic forces.

One of the difficulties in solving such two-way coupled problems is that standard Newton methods (for solving the nonlinear algebraic equations associated with either

*This work was supported in part by Algor, Inc. Computations were performed on computers purchased with funds provided in part by NSF equipment grant BCS-9212819.

†Computational Mechanics Laboratory, Department of Civil and Environmental Engineering, Carnegie Mellon University, Pittsburgh, Pennsylvania, 15213, USA (oghattas@cs.cmu.edu).

‡Algor, Inc., 150 Beta Drive, Pittsburgh, Pennsylvania, 15238, USA (xli@algor.com.)

the steady problem or each time step of the transient problem) produce linear systems at each iteration that are difficult to solve. Difficulties arise because the coefficient matrix of these systems—the Jacobian matrix of the residual equations—is either too large, too ill-conditioned, or too unstructured for existing solution techniques. As a result, most algorithms for coupled multidomain problems iterate back and forth between single-domain solvers, for example alternating between the solution of (possibly linearized) fluid equations followed by (possibly linearized) solid ones, with the goal of iterating toward a steady state in the case of the steady problem, or tracing a time history in the case of the transient problem. While true Newton methods—which directly attack the coupled Jacobian—are expected to require fewer iterations than such so-called *segregated* solvers, the desire to make use of existing fluid and solid discretization schemes, solution algorithms, and software motivates the popularity of segregated methods for aeroelasticity problems [5], [10], [21], [14], [15], [16], [17]. By decomposing into separate subproblems, one is often able to exploit the properties of single-domain operators. Nevertheless, one would like to enjoy the fast convergence of Newton methods—which means having to "invert" the fully coupled Jacobian—but at the same time retain segregated solvers' ability to exploit properties of single-domain solvers.

Unfortunately, sensitivity analysis is not kind to segregated solvers. It is well known that the sensitivity of the state variables to a design parameter can be found by solving a linear system of equations, whose coefficient matrix is the Jacobian of the nonlinear residual, and whose righthand side is the derivative of the residual with respect to that parameter.[1] Thus, sensitivity analysis requires solution of a system of equations having the same coefficient matrix needed by Newton's method for solving the state equations—a solution technique that most multidomain solvers seek to avoid. How to reconcile these conflicting desires? One could of course differentiate (with respect to design parameters) the nonlinear iterative process for solving the state equations, but this is surely inefficient, since the cost of obtaining each sensitivity would be equal to the cost of solving the state equations. Finite-differencing is equally inefficient, since again the cost is of the order of the cost of state equation solution (with some savings due to having available good initial guesses). One would like to exploit the fact that the sensitivity equations are linear, even if the state equations are nonlinear.

In this paper we develop methods for solution and sensitivity analysis of a finite element approximation of the aeroelasticity problem defined above. These methods combine the convenience of segregated solvers with the efficiency of coupled methods. The solution methods combine the speed of Newton-like methods with the ability to exploit separate solid and fluid solvers. The sensitivity methods directly attack the linear sensitivity equations without forming the coupled Jacobian, and also exploit separate solid and fluid solvers. In fact, the solution and sensitivity methods are closely related, and make use of the same basic components. Roughly speaking, the central idea is to retain the two-way coupling within the framework of a (coupled Jacobian) matrix-free iterative solver, but introduce one-way coupled fluid and solid solves as a preconditioner.

The solution and sensitivity analysis methods presented here are of domain-decomposition type, in the sense that they make use of preconditioners that decompose into separate problems posed on distinct domains. These domains are simply

[1] Sobieski has termed this approach GSE1; for an alternative approach, known as GSE2, we refer the reader to [23].

the solid and fluid domains. We use a conforming finite element approximation and direct sparse factorization on both the solid and fluid domains; however, any suitable discretization method and linear system solver could have been used. The domain decomposition preconditioners can be viewed as nonoverlapping block Gauss–Seidel methods, although the splitting discards some diagonal terms as well. These preconditioners are thus of the multiplicative type.

The remainder of the paper is organized as follows. The stationary nonlinear aeroelasticity problem is defined in §2. In §3, we formulate the coupled problem variationally in a way that couples solid and fluid prior to numerical approximation, and that insures continuity of interface tractions. The translation of the variational formulation into a unified finite element method is also presented in §3. The finite element method produces a single set of nonlinear algebraic equations describing the interaction of solid and fluid. Special treatment is required to solve this system efficiently. Thus, in §4, two Newton-like solution methods for the coupled discrete problem are proposed that make use of a decomposition into separate fluid and solid domain solves. The first is a domain-decomposed approximate Newton method, and the second is a Newton-Krylov method with domain-decomposition preconditioning. These two solution methods form the basis for two closely-related sensitivity analysis methods, which are described in §5. The first is a stationary iterative method that makes use of domain decomposition preconditioning, and the second is a Krylov method with domain-decomposition preconditioning. In §6, the methodology presented in this paper is illustrated on a problem of the flow-induced large deformation of an elastic cylinder.

For an introduction to sensitivity analysis, both discrete and continuous, the reader is referred to [18, Chapters 7 & 8]. A set of references spanning the field of multidisciplinary design optimization can be found in the series of proceedings [1], [2], [3], as well as the recent collection [4]. In particular, a comprehensive summary of advances in sensitivity analysis of nonlinear solid mechanics problems can be found in [6]. For an overview of sensitivity and optimization of incompressible Navier-Stokes flows, we recommend [13].

2. Governing equations of the stationary problem. Consider a system composed of a solid of finite extent, surrounded by a fluid of infinite extent. We assume that the fluid is viscous, incompressible, and Newtonian, and thus is governed by the Navier-Stokes equations. The solid is taken to be isotropic and elastic, and is assumed to undergo large displacements but small strains. Table 2.1 displays definitions of the symbols representing the domains, interfaces, boundaries, fluid and solid field quantities, material constants, and prescribed data. Figure 2.1 depicts the problem.

If $\mathbf{v}$ is a vector and $\mathbf{S}$ a tensor, then the components of the tensor $\boldsymbol{\nabla}\mathbf{v}$ and the vector $\mathbf{div}\,\mathbf{S}$ are given by

$$(\boldsymbol{\nabla}\mathbf{v})_{ij} = \frac{\partial v_j}{\partial x_i}, \qquad (\mathbf{div}\,\mathbf{S})_i = \sum_i \frac{\partial S_{ij}}{\partial x_j},$$

where $\boldsymbol{\nabla}$ and $\mathbf{div}$ are respectively the spatial gradient and spatial divergence with respect to a cartesian reference frame. The constitutive law, equilibrium equations, and strain-displacement relations of the solid, in Lagrangian form, are given by

$$\mathbf{S} = \lambda_S \mathrm{tr}(\mathbf{E})\mathbf{I} + 2\mu_S \mathbf{E} \qquad \text{in } \Omega_S, \tag{2.1}$$

$$\mathbf{div}\left[(\mathbf{I} + \boldsymbol{\nabla}\mathbf{u})\,\mathbf{S}\right] = \mathbf{f}_S \qquad \text{in } \Omega_S, \tag{2.2}$$

TABLE 2.1
Definitions of symbols

Domains, interfaces, and boundaries	
Ω	domain of the combined solid and fluid system
Ω_S	domain occupied by the undeformed solid
Ω_F	domain occupied by the fluid
Γ_S^1	portion of the undeformed solid boundary on which tractions are prescribed
Γ_S^2	portion of the undeformed solid boundary on which displacements are prescribed
Γ_F^1	portion of the fluid far-field boundary on which tractions are prescribed
Γ_F^2	portion of the far-field fluid boundary on which velocity is prescribed
Γ_{I_0}	interface between undeformed solid and fluid
Γ_I	interface between deformed solid and fluid
$\mathbf{n}$	outward unit normal to a deformed surface
$\mathbf{n}_{I_S}$	unit normal to the interface between deformed solid and fluid, directed away from the solid
$\mathbf{n}_{I_F}$	unit normal to the interface between deformed solid and fluid, directed away from the fluid
$\mathbf{n}_0$	outward unit normal to an undeformed surface
Fluid and solid field quantities	
$\mathbf{u}$	solid displacement vector
$\mathbf{S}$	solid second Piola-Kirchhoff stress tensor
$\mathbf{E}$	solid Green strain tensor
$\boldsymbol{\sigma}_S$	solid Cauchy (Eulerian) stress tensor
p	fluid pressure
$\mathbf{v}$	fluid velocity vector
$\boldsymbol{\sigma}_F$	fluid stress tensor
$\mathbf{d}$	fluid rate of strain tensor
Material constants and prescribed data	
λ_S, μ_S	Lamé moduli of the solid
μ_F	fluid viscosity
ρ_F	fluid density
$\mathbf{f}_S$	solid body force in an undeformed configuration
$\mathbf{f}_F$	fluid body force
$\hat{\mathbf{u}}$	prescribed solid displacement
$\hat{\mathbf{t}}_S$	prescribed solid traction
$\hat{\mathbf{v}}$	prescribed far-field fluid velocity
$\hat{\mathbf{t}}_F$	prescribed fluid traction

$$\mathbf{E} = \frac{1}{2}\left[\boldsymbol{\nabla}\mathbf{u} + \boldsymbol{\nabla}\mathbf{u}^T + \boldsymbol{\nabla}\mathbf{u}\boldsymbol{\nabla}\mathbf{u}^T\right] \qquad \text{in } \Omega_S. \tag{2.3}$$

As a consequence of the small strain assumption, we are able to use a linear constitutive relationship (2.1) for the solid. The conservation of momentum, conservation of mass, constitutive law, and strain rate-velocity equations of the fluid, in Eulerian form, are

$$\rho_F(\mathbf{v}\cdot\boldsymbol{\nabla})\mathbf{v} - \mathbf{div}\,\boldsymbol{\sigma}_F = \mathbf{f}_F \qquad \text{in } \Omega_F, \tag{2.4}$$

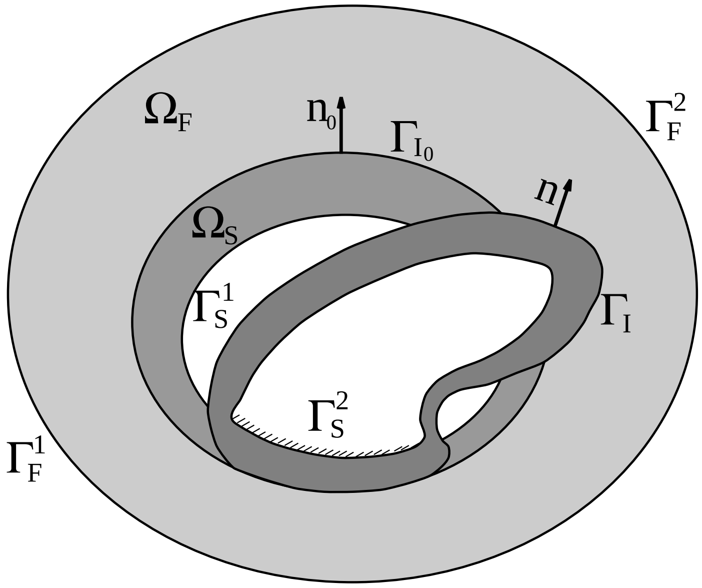

FIG. 2.1. *Nonlinear aeroelasticity problem.*

$$\nabla \cdot \mathbf{v} = 0 \qquad \text{in } \Omega_F, \tag{2.5}$$

$$\boldsymbol{\sigma}_F = -p\mathbf{I} + 2\mu_F \mathbf{d} \qquad \text{in } \Omega_F, \tag{2.6}$$

$$\mathbf{d} = \frac{1}{2}\left(\nabla \mathbf{v} + \nabla \mathbf{v}^T\right) \qquad \text{in } \Omega_F. \tag{2.7}$$

Coupling between fluid and solid requires that traction and velocity be continuous on the deformed interface:

$$\boldsymbol{\sigma}_S \mathbf{n}_{I_S} + \boldsymbol{\sigma}_F \mathbf{n}_{I_F} = \mathbf{0} \qquad \text{on } \Gamma_I, \tag{2.8}$$

$$\mathbf{v} = \dot{\mathbf{u}} = \mathbf{0} \qquad \text{on } \Gamma_I, \tag{2.9}$$

where, under the assumption that density changes due to deformation are negligible (valid if strains are small as assumed), the Cauchy stress in the solid is given by $\boldsymbol{\sigma}_S = (\mathbf{I} + \nabla \mathbf{u})\mathbf{S}(\mathbf{I} + \nabla \mathbf{u}^T)$. Here, $\dot{\mathbf{u}}$ is the solid velocity, which is zero due to the steady state nature of the problem. This stationary assumption effectively yields a no-slip condition on the fluid velocity field on the interface. Finally, the boundary conditions take the form

$$\boldsymbol{\sigma}_F \mathbf{n}_F = \hat{\mathbf{t}}_F \qquad \text{on } \Gamma_F^1, \tag{2.10}$$

$$\left[(\mathbf{I} + \nabla \mathbf{u})\,\mathbf{S}\right]\mathbf{n}_0 = \hat{\mathbf{t}}_S \qquad \text{on } \Gamma_S^1, \tag{2.11}$$

$$\mathbf{v} = \hat{\mathbf{v}} \qquad \text{on } \Gamma_F^2, \tag{2.12}$$

$$\mathbf{u} = \hat{\mathbf{u}} \qquad \text{on } \Gamma_S^2. \tag{2.13}$$

In the next section we give the variational form and a finite element approximation of the coupled fluid-solid problem. In the sequel, we assume, without loss of generality, that fluid and solid experience neither body forces nor surface tractions, i.e. $\mathbf{f}_F$, $\mathbf{f}_S$, $\hat{\mathbf{t}}_f$, and $\hat{\mathbf{t}}_S$ are all zero.

3. Variational form and finite element approximation. In [11] we derive a variational formulation of the viscous flow-finite elasticity interaction problem defined above. This formulation of course is not a classical variational form; it does not derive from stationarity of any functional. It is a weak form of the governing equations, that automatically satisfies the continuity of interface tractions; we use the term *variational* in this sense.

Here we state the variational formulation without proof; see [11] for details. First, let us define the following functionals:

$$a(\mathbf{v}, \mathbf{w}) = \int_{\Omega_F} \frac{\mu_F}{2} \left(\boldsymbol{\nabla}\mathbf{v} + \boldsymbol{\nabla}\mathbf{v}^T\right) : \left(\boldsymbol{\nabla}\mathbf{w} + \boldsymbol{\nabla}\mathbf{w}^T\right) d\Omega_F(\mathbf{u}), \tag{3.1}$$

$$b(p, \mathbf{w}) = -\int_{\Omega_F} p \boldsymbol{\nabla} \cdot \mathbf{w} \; d\Omega_F(\mathbf{u}), \tag{3.2}$$

$$c(\mathbf{v}, \mathbf{v}, \mathbf{w}) = \int_{\Omega_F} \rho_F \mathbf{w} \cdot (\mathbf{v} \cdot \boldsymbol{\nabla})\, \mathbf{v} \; d\Omega_F(\mathbf{u}), \tag{3.3}$$

$$d(\mathbf{u}, \mathbf{r}) = \int_{\Omega_S} \boldsymbol{\nabla}\mathbf{r} : \mathbf{S}^L(\mathbf{u}) \; d\Omega_S, \tag{3.4}$$

$$e(\mathbf{u}, \mathbf{u}, \mathbf{r}) = \int_{\Omega_S} \boldsymbol{\nabla}\mathbf{r} : \left[\mathbf{S}^N(\mathbf{u}) + \boldsymbol{\nabla}\mathbf{u}\, \mathbf{S}^L(\mathbf{u})\right] d\Omega_S, \tag{3.5}$$

$$f(\mathbf{u}, \mathbf{u}, \mathbf{u}, \mathbf{r}) = \int_{\Omega_S} \boldsymbol{\nabla}\mathbf{r} : \left[\boldsymbol{\nabla}\mathbf{u}\, \mathbf{S}^N(\mathbf{u})\right] \; d\Omega_S, \tag{3.6}$$

where the symbol : denotes the scalar product of two tensors, i.e.

$$\mathbf{S} : \mathbf{T} = \sum_{i,j} S_{ij} T_{ij}.$$

The solid stress tensor has been split into $\mathbf{S}^L$, a tensor that depends linearly on displacement gradient, and $\mathbf{S}^N$, one that depends nonlinearly, i.e.,

$$\mathbf{S}^L = \lambda_S \operatorname{tr}(\boldsymbol{\nabla}\mathbf{u})\, \mathbf{I} + \mu_S \left(\boldsymbol{\nabla}\mathbf{u} + \boldsymbol{\nabla}\mathbf{u}^T\right), \tag{3.7}$$

$$\mathbf{S}^N = \frac{1}{2} \lambda_S \operatorname{tr}\left(\boldsymbol{\nabla}\mathbf{u} \boldsymbol{\nabla}\mathbf{u}^T\right) \mathbf{I} + \mu_S \left(\boldsymbol{\nabla}\mathbf{u} \boldsymbol{\nabla}\mathbf{u}^T\right), \tag{3.8}$$

so that $\mathbf{S} = \mathbf{S}^L + \mathbf{S}^N$. The first three functionals arise from the conservation of momentum equation in the fluid: $a(\mathbf{v}, \mathbf{w})$ is a weak form of the viscous term , $b(p, \mathbf{w})$

is a weak form of the pressure gradient term, and $c(\mathbf{v}, \mathbf{v}, \mathbf{w})$ is a weak form of the convective term. Note the dependence of the domain of integration of the fluid functionals on displacement of the solid. This is a consequence of the large displacement nature of the problem. The remaining three functionals stem from the solid equilibrium equation: $d(\mathbf{u}, \mathbf{r})$ is a weak form of the portion of the stress divergence term that is linear in displacement gradient, $e(\mathbf{u}, \mathbf{u}, \mathbf{r})$ is a weak form of the quadratic portion, and $f(\mathbf{u}, \mathbf{u}, \mathbf{u}, \mathbf{r})$ is a weak form of the cubic portion.

We define the following spaces: $\mathbf{H}_0^1(\Omega_F)$ is the Sobolev subspace of all functions having one square integrable derivative over Ω_F and that vanish on Γ_F^2 and in Ω_S, $L^2(\Omega_F)$ is the space of functions that are square integrable over Ω_F and that vanish in Ω_S, and $\mathbf{H}_0^1(\Omega_S)$ is the Sobolev subspace of all functions having one square integrable derivative over Ω_S and that vanish on Γ_S^2 and in Ω_F. The variational form of the problem can now be stated as: Find $\mathbf{v} \in \mathbf{H}_0^1(\Omega)$, $p \in L^2(\Omega)$, and $\mathbf{u} \in \mathbf{H}_0^1(\Omega)$ such that

$$\begin{aligned} &a(\mathbf{v}, \mathbf{w}) + b(p, \mathbf{w}) + c(\mathbf{v}, \mathbf{v}, \mathbf{w}) + d(\mathbf{u}, \mathbf{r}) + e(\mathbf{u}, \mathbf{u}, \mathbf{r}) + f(\mathbf{u}, \mathbf{u}, \mathbf{u}, \mathbf{r}) = 0 \\ &\qquad\qquad \text{for all } \mathbf{w} \in \mathbf{H}_0^1(\Omega_F) \text{ and } \mathbf{r} \in \mathbf{H}_0^1(\Omega_S), \end{aligned} \tag{3.9}$$

$$b(q, \mathbf{v}) = 0 \qquad \text{for all } q \in L^2(\Omega_F). \tag{3.10}$$

The essential boundary conditions $\mathbf{v} = \hat{\mathbf{v}}$ and $\mathbf{u} = \hat{\mathbf{u}}$ must be enforced on Γ_F^2 and Γ_S^2, respectively. In addition, the continuity of interface velocity condition (2.9), and consequently a no-slip condition, must be enforced on the fluid velocity field along the solid-fluid interface. There is one final condition that arises in the derivation of the variational form (3.9)–(3.10): the test functions for solid and fluid, $\mathbf{r}$ and $\mathbf{w}$, must agree when restricted to the interface [11]. By appropriate application of the divergence theorem, and by recognition of the relationship between interface surface tractions expressed in terms of Cauchy and Kirchhoff stresses, one may verify that the variational form (3.9)–(3.10) is equivalent to the strong form of the governing equations (2.1)–(2.13) [11]. This variational form automatically satisfies continuity of fluid-solid interface tractions.

It is straightforward to translate the variational form into a finite element approximation. We introduce the finite element spaces $\mathcal{V}_h$, $\mathcal{P}_h$, and $\mathcal{U}_h$ for velocity, pressure, and displacement, respectively. We assume that the finite element spaces are conforming, i.e. the finite element spaces $\mathcal{V}_h$, $\mathcal{P}_h$, and $\mathcal{U}_h$ are subspaces of the infinite dimensional spaces in (3.9) and (3.10),

$$\mathcal{V}_h \subset \mathbf{H}_0^1(\Omega_F), \quad \mathcal{P}_h \subset L_0^2(\Omega_F), \quad \mathcal{U}_h \subset \mathbf{H}_0^1(\Omega_S).$$

The Galerkin method restricts the variational problem to these finite-dimensional subspaces, and yields the following discrete problem: Find $\mathbf{v}_h \in \mathcal{V}_h$, $p_h \in \mathcal{P}_h$, and $\mathbf{u}_h \in \mathcal{U}_h$ such that

$$\begin{aligned} &a(\mathbf{v}_h, \mathbf{w}_h) + b(p_h, \mathbf{w}_h) + c(\mathbf{v}_h, \mathbf{v}_h, \mathbf{w}_h) + d(\mathbf{u}_h, \mathbf{r}_h) + e(\mathbf{u}_h, \mathbf{u}_h, \mathbf{r}_h) \\ &\qquad + f(\mathbf{u}_h, \mathbf{u}_h, \mathbf{u}_h, \mathbf{r}_h) = 0 \quad \text{for all } \mathbf{w}_h \in \mathcal{V}_h \text{ and } \mathbf{r}_h \in \mathcal{S}_h, \end{aligned} \tag{3.11}$$

$$b(q, \mathbf{v}_h) = 0 \qquad \text{for all } q \in \mathcal{P}_h. \tag{3.12}$$

In particular, let the finite element spaces be spanned by the basis function families $\boldsymbol{\psi}_i$, $\boldsymbol{\phi}_j$, and χ_k:

$$\mathcal{U}_h = \operatorname{span}\{\boldsymbol{\psi}_1, \ldots, \boldsymbol{\psi}_{n^u}\}, \tag{3.13}$$

$$\mathcal{V}_h = \text{ span}\left\{\boldsymbol{\phi}_1, \ldots, \boldsymbol{\phi}_{n^v}\right\}, \tag{3.14}$$

$$\mathcal{P}_h = \text{ span}\left\{\chi_1, \ldots, \chi_{n^p}\right\}, \tag{3.15}$$

where n^u is the number of displacement nodes, n^v is the number of velocity nodes, and n^p is the number of pressure nodes. Thus, the approximations $\mathbf{u}_h$, $\mathbf{v}_h$, and p_h for displacement, velocity, and pressure, respectively, are given by

$$\mathbf{u}_h = \sum_{k=1}^{n^u} \boldsymbol{\psi}_k(\mathbf{x}) u_k, \tag{3.16}$$

$$\mathbf{v}_h = \sum_{i=1}^{n^v} \boldsymbol{\phi}_i(\mathbf{x}) v_i, \tag{3.17}$$

$$p_h = \sum_{j=1}^{n^p} \chi_j(\mathbf{x}) p_j. \tag{3.18}$$

The choices of the finite element spaces may not be arbitrary. First, the pair of spaces $\mathcal{V}_h$ and $\mathcal{P}_h$ must satisfy the Ladyzhenskaya-Babuska-Brezzi stability condition [12]. Second, the requirement that displacement and velocity test functions be identical when restricted to the interface is satisfied by insisting that $\mathcal{U}_h$ and $\mathcal{V}_h$ match at the interface [11].

The discrete problem (3.11)–(3.12) is a system of nonlinear algebraic equations. Let n_S^u denote the number of displacement nodes lying strictly in Ω_S as well as on Γ_S^1, n_F^v the number of velocity nodes lying strictly in Ω_F as well as on Γ_F^1, n_F^p the number of pressure nodes lying strictly in Ω_F, n_I^s the number of displacement nodes lying on Γ_{I_0}, n_I^v the number of velocity nodes lying on Γ_I, and n_I^p the number of pressure nodes lying on Γ_I. Therefore,

$$\begin{aligned} n^v &= n_F^v + n_I^v \\ n^p &= n_F^p + n_I^p \\ n^u &= n_S^u + n_I^u \end{aligned} \tag{3.19}$$

Our insistence that $\mathcal{U}_h$ and $\mathcal{V}_h$ agree on the interface implies that the number of displacement interface nodes n_I^u and the number of velocity interface nodes n_I^v are equal; let us call this common number n_I. Let the velocity nodes be ordered such that nodes $1, \ldots, n_I$ lie on the interface and $n_I + 1, \ldots, n^v$ lie in the fluid domain as well as that portion of the fluid boundary on which tractions are prescribed. Similarly, the velocity nodes are ordered such that nodes $1, \ldots, n_I$ lie on the interface and $n_I + 1, \ldots, n^u$ lie in the solid domain as well as that portion of the solid boundary on which tractions are prescribed.

We can now explicitly state the system of nonlinear algebraic equations corresponding to the discrete problem (3.11)–(3.12). In the fluid, we have the n_F^v discrete conservation of momentum equations

$$\begin{aligned} \sum_{i=1}^{n^v} a(\boldsymbol{\phi}_i, \boldsymbol{\phi}_\ell) v_i + \sum_{j=1}^{n^p} b(\chi_j, \boldsymbol{\phi}_\ell) p_j + \sum_{i,r=1}^{n^v} c(\boldsymbol{\phi}_i, \boldsymbol{\phi}_r, \boldsymbol{\phi}_\ell) v_i v_r = 0, \\ \ell = n_I + 1, \ldots, n^v, \end{aligned} \tag{3.20}$$

and the n_F^p discrete conservation of mass equations

$$\sum_{i=1}^{n^v} b(\chi_m, \boldsymbol{\phi}_i) v_i = 0, \quad m = n_I^p, \dots, n^p. \tag{3.21}$$

In the solid, the n_S^u discrete equilibrium equations take the form

$$\sum_{k=1}^{n^u} d(\boldsymbol{\psi}_k, \boldsymbol{\psi}_n) u_k + \sum_{k,s=1}^{n^u} e(\boldsymbol{\psi}_k, \boldsymbol{\psi}_s, \boldsymbol{\psi}_n) u_k u_s + \sum_{k,s,t=1}^{n^u} f(\boldsymbol{\psi}_k, \boldsymbol{\psi}_s, \boldsymbol{\psi}_t, \boldsymbol{\psi}_n) u_k u_s u_t = 0, \qquad n = n_I + 1, \dots, n^u. \tag{3.22}$$

Finally, on the interface, we obtain the n_I discrete traction continuity equations

$$\begin{aligned} &\sum_{i=1}^{n^v} a(\boldsymbol{\phi}_i, \boldsymbol{\phi}_y) v_i + \sum_{j=1}^{n^p} b(\chi_j, \boldsymbol{\phi}_y) p_j + \sum_{i,r=1}^{n^v} c(\boldsymbol{\phi}_i, \boldsymbol{\phi}_r, \boldsymbol{\phi}_y) v_i v_r + \sum_{k=1}^{n^u} d(\boldsymbol{\psi}_k, \boldsymbol{\psi}_y) u_k \\ &+ \sum_{k,s=1}^{n^u} e(\boldsymbol{\psi}_k, \boldsymbol{\psi}_s, \boldsymbol{\psi}_y) u_k u_s + \sum_{k,s,t=1}^{n^u} f(\boldsymbol{\psi}_k, \boldsymbol{\psi}_s, \boldsymbol{\psi}_t, \boldsymbol{\psi}_y) u_k u_s u_t = 0, \quad y = 1, \dots, n_I, \end{aligned} \tag{3.23}$$

and the n_I^p discrete conservation of mass equations

$$\sum_{i=1}^{n^v} b(\chi_z, \boldsymbol{\phi}_i) v_i = 0 \qquad z = 1, \dots, n_I^p. \tag{3.24}$$

Equations (3.20)–(3.24) are a system of $n^v + n^p + n^u - n_I$ nonlinear equations in $n^v + n^p + n^u$ unknowns. Upon requiring that fluid velocities vanish on the interface as implied by the continuity of interface velocity condition (2.9), we obtain n_I fewer unknowns, and thus we arrive at an equal number of equations and unknowns.

We emphasize that not only do the solid equilibrium equations (3.22) depend on the interface displacements, but so do the fluid conservation of momentum (3.20) and mass (3.21) equations, as well as the interface traction continuity equations (3.23) and interface conservation of mass (3.24). This results from the dependence of the domains of integration of the functionals $a(\cdot,\cdot)$, $b(\cdot,\cdot)$, and $c(\cdot,\cdot,\cdot)$ on the interface displacement, i.e. in the dependence of the flow on interface geometry. These create special difficulties for the solver that must be overcome.

4. Domain decomposition methods for solution of the discrete system. In this section we develop two domain decomposition methods for solving the nonlinear algebraic equations representing the coupled fluid-solid system. These methods combine the ability of segregated solvers to invoke disciplinary (fluid and solid) solvers while maintaining the advantages of coupled solution (rigorous treatment of interface conditions, faster convergence). Furthermore, these domain decomposition methods form the basis for the two sensitivity equation solvers presented in the next section.

Let us begin by grouping the fluid nodal velocities, fluid nodal pressures, and interface nodal pressures together as a single vector of unknowns, which we term the *fluid unknowns*,

$$\mathbf{x}_F \in \Re^{n_F}, \quad n_F = n_F^v + n_F^p + n_I^p.$$

The *solid unknowns*,

$$\mathbf{x}_S \in \Re^{n_S}, \quad n_S = n_S^u,$$

are comprised of the solid nodal displacements. Finally, the interface displacements constitute the *interface unknowns*,

$$\mathbf{x}_I \in \Re^{n_I}.$$

Note that we have chosen to include the interface pressures among the velocity unknowns, for reasons that will become apparent soon. Furthermore, interface velocities have been set to zero as a consequence of the interface velocity continuity condition (2.9) and thus do not appear as unknowns. We now proceed to write the discrete fluid-solid interaction equations (3.20)–(3.24) symbolically as

$$\begin{aligned} \mathbf{h}_F\left(\mathbf{x}_F, \mathbf{x}_I\right) &= 0 \\ \mathbf{h}_S\left(\mathbf{x}_S, \mathbf{x}_I\right) &= 0 \\ \mathbf{h}_I\left(\mathbf{x}_F, \mathbf{x}_S, \mathbf{x}_I\right) &= 0 \end{aligned} \tag{4.1}$$

Here, the *fluid residual* vector $\mathbf{h}_F \in \Re^{n_F}$ includes the fluid conservation of momentum residual from (3.20), the fluid conservation of mass residual from (3.21), and the interface conservation of mass residual from (3.24). The reason for including interface conservation of mass in the fluid residual will again become apparent. The *solid residual* vector $\mathbf{h}_S \in \Re^{n_S}$ is composed of the residual of the solid equilibrium equations (3.22), while the *interface residual* vector $\mathbf{h}_I \in \Re^{n_I}$ corresponds to the residual of the discrete continuity of interface traction equations (3.23).

The two methods for solving (4.1) we develop are Newton-like methods. Given an initial iterate $\mathbf{x}^0$, Newton's method for the nonlinear system $\mathbf{h}(\mathbf{x}) = 0$ consists of iterating on solution of the linear system

$$\mathbf{J}(\mathbf{x}^k)(\mathbf{x}^{k+1} - \mathbf{x}^k) = -\mathbf{h}(\mathbf{x}^k) \tag{4.2}$$

until convergence, where $\mathbf{J}$ is the Jacobian matrix of $\mathbf{h}$ with respect to $\mathbf{x}$, and is in general unsymmetric and indefinite. A Newton step for the discrete system (4.1) takes the form

$$\begin{bmatrix} \mathbf{J}_{FF}^k & \mathbf{0} & \mathbf{J}_{FI}^k \\ \mathbf{0} & \mathbf{J}_{SS}^k & \mathbf{J}_{SI}^k \\ \mathbf{J}_{IF}^k & \mathbf{J}_{IS}^k & \mathbf{J}_{II_F}^k + \mathbf{J}_{II_S}^k \end{bmatrix} \begin{Bmatrix} \Delta\mathbf{x}_F \\ \Delta\mathbf{x}_S \\ \Delta\mathbf{x}_I \end{Bmatrix} = - \begin{Bmatrix} \mathbf{h}_F^k \\ \mathbf{h}_S^k \\ \mathbf{h}_I^k \end{Bmatrix}, \tag{4.3}$$

where

$$\Delta\mathbf{x} = \mathbf{x}^{k+1} - \mathbf{x}^k \tag{4.4}$$

and the superscript k indicates evaluation of the residual $\mathbf{h}$ and the Jacobian $\mathbf{J}$ at the point $\mathbf{x}^k$. In (4.3), the interface-interface coupling matrix $\mathbf{J}_{II}$ has been split into contributions from both solid and fluid,

$$\mathbf{J}_{II} = \mathbf{J}_{II_F} + \mathbf{J}_{II_S}. \tag{4.5}$$

The Newton iteration (4.3) entails two difficulties: First, the Jacobian matrix, because of the disparity between fluid and solid properties, can be very ill-conditioned.

Second, the coupling terms between fluid and interface variables in general render the matrices $\mathbf{J}_{FI}$ and $\mathbf{J}_{II_F}$ dense. The density of these matrices is a consequence of the dependence of the domains of integration of the fluid functionals $a(\cdot,\cdot)$, $b(\cdot,\cdot)$, and $c(\cdot,\cdot,\cdot)$ on the interface displacements.[2] In the case of $\mathbf{J}_{FI}$, all fluid nodal velocities and pressures may be coupled to all interface nodal displacements, since a change in any interface displacement potentially moves the fluid mesh everywhere. The matrix $\mathbf{J}_{II_F}$ derives its density from the fact that the interface traction continuity equation (3.23) includes contributions from the first layer of fluid elements, which change with a movement in the interface. Thus, the potential exists for coupling between all interface variables. $\mathbf{J}_{II_S}$ contains nonzeroes contributed by the solid terms in (3.23), i.e. the terms involving $d(\cdot,\cdot)$, $e(\cdot,\cdot,\cdot)$, and $f(\cdot,\cdot,\cdot,\cdot)$. These are just the standard solid stiffness coupling terms, so the coupling is local in nature. The exact sparsity depends on the moving mesh scheme employed, but in general, the storage requirements and arithmetic complexity associated with $\mathbf{J}_{FI}$ and $\mathbf{J}_{II_F}$ can be quite severe.

In the remainder of this section, we introduce two domain decomposition Newton-like methods to alleviate the difficulties of density and ill-conditioning described above. The first method is a domain-decomposed approximate Newton method that assumes one-way coupling to allow separate fluid and solid solves. It can be thought of as a fixed point method with domain decomposition preconditioning. The second method uses Newton-Krylov ideas and a domain decomposition preconditioner based on a one-way coupling assumption. Both of these solution techniques form the basis for the sensitivity equations solvers presented in §5.

4.1. Solution Method I (SOM1): A domain-decomposed approximate Newton method. Our first Newton-like method is an *approximate* Newton method obtained by ignoring the two dense coupling matrices: $\mathbf{J}_{FI}$, the fluid-interface coupling matrix, and $\mathbf{J}_{II_F}$, the contribution of the fluid to the interface-interface coupling matrix. The resulting Jacobian in (4.3) becomes block-lower triangular. Thus, the fluid variables can be found by solving the linearized fluid problem

$$\mathbf{J}^k_{FF}\Delta\mathbf{x}_F = -\mathbf{h}^k_F \tag{4.6}$$

for $\Delta\mathbf{x}_F$. The change in the displacements (both interior and interface) can then be found by solving the linearized solid problem

$$\begin{bmatrix} \mathbf{J}^k_{SS} & \mathbf{J}^k_{SI} \\ \mathbf{J}^k_{IS} & \mathbf{J}^k_{II_S} \end{bmatrix} \begin{Bmatrix} \Delta\mathbf{x}_S \\ \Delta\mathbf{x}_I \end{Bmatrix} = - \begin{Bmatrix} \mathbf{h}^k_S \\ \mathbf{h}^k_I + \mathbf{J}^k_{IF}\Delta\mathbf{x}_F \end{Bmatrix}. \tag{4.7}$$

The fluid step (4.6) can be seen to be simply a Newton step for the Navier-Stokes equations, with a rigid boundary given by the current position of the deformed interface, and a no-slip boundary condition imposed on it (this is why the interface pressures are included among the set of fluid unknowns). The solid step (4.7) can be regarded also as a Newton step, for the solid equilibrium equations. The term $\mathbf{J}^k_{IF}\Delta\mathbf{x}_F$ is the incremental "loading" that the linearized fluid problem induces on the solid through the interface. So at a typical Newton-like iteration, we first solve a linearized fluid problem, then communicate the effective tractions it induces to the interface, and finally solve a linearized solid problem under this loading.

Effectively, this approximate Jacobian replaces the two-way coupling arising from geometric dependence of the fluid domain on solid displacements, with one-way coupling. This one-way coupling avoids ill-conditioning associated with the two-way

[2]Note that these matrices would be zero if an infinitesimal displacement approximation were made, i.e. if we assumed that the fluid domain of definition was independent of the solid deformation.

coupled exact Jacobian, by allowing distinct fluid and solid solves. As an additional advantage, the large storage requirement associated with geometric coupling matrices is avoided by ignoring these terms while constructing the Jacobian.

We stress that the use of this one-way-coupled approximate Jacobian is only a numerical device for solving the system of nonlinear equations (4.1). Since the residual in (4.3) is calculated correctly, we are guaranteed that, if the method converges, it must converge to the correct solution. This can be seen from (4.2): the only way that $\Delta\mathbf{x}$ can be zero is for $\mathbf{h}$ to be zero, provided only that $\mathbf{J}$ is nonsingular, regardless of whether or not it represents the true Jacobian. The price we pay for this approximate Jacobian is that we must give up the Newton guarantee of local quadratic convergence. Instead, local linear convergence to a solution $\mathbf{x}^*$ is assured if

$$\rho\left(\mathbf{I} - \tilde{\mathbf{J}}\left(\mathbf{x}^*\right)^{-1}\mathbf{J}\left(\mathbf{x}^*\right)\right) < 1, \tag{4.8}$$

where ρ is the spectral radius and $\tilde{\mathbf{J}}$ is the approximate Jacobian obtained by ignoring $\mathbf{J}_{FI}$ and $\mathbf{J}_{II_F}$, i.e.

$$\tilde{\mathbf{J}} = \begin{bmatrix} \mathbf{J}_{FF} & \mathbf{0} & \mathbf{0} \\ \mathbf{0} & \mathbf{J}_{SS} & \mathbf{J}_{SI} \\ \mathbf{J}_{IF} & \mathbf{J}_{IS} & \mathbf{J}_{II_S} \end{bmatrix}. \tag{4.9}$$

Condition (4.8) is a standard result in the theory of methods of Newton form, e.g. [20]. It is easy to show that

$$\tilde{\mathbf{J}}^{-1}\mathbf{J} = \begin{bmatrix} \mathbf{I} & \mathbf{0} & \mathbf{J}_{FF}^{-1}\mathbf{J}_{FI} \\ \mathbf{0} & \mathbf{I} & -\mathbf{J}_{SS}^{-1}\mathbf{J}_{SI}\mathbf{S}_S^{-1}\mathbf{S}_F \\ \mathbf{0} & \mathbf{0} & \mathbf{I} + \mathbf{S}_S^{-1}\mathbf{S}_F \end{bmatrix}, \tag{4.10}$$

where

$$\mathbf{S}_S = \mathbf{J}_{IS}\mathbf{J}_{SS}^{-1}\mathbf{J}_{SI} - \mathbf{J}_{II_S},$$

$$\mathbf{S}_F = \mathbf{J}_{IF}\mathbf{J}_{FF}^{-1}\mathbf{J}_{FI} - \mathbf{J}_{II_F}.$$

So condition (4.8) reduces to

$$\rho\left(\mathbf{S}_S^{-1}\mathbf{S}_F\right) < 1. \tag{4.11}$$

The matrix $\mathbf{S} = \mathbf{S}_S + \mathbf{S}_F$ is the Schur complement of the interface-interface coupling matrix $\mathbf{J}_{II}$ in the Jacobian $\mathbf{J}$; $\mathbf{S}_S$ is the contribution of the solid to this Schur complement, and $\mathbf{S}_F$ is the fluid contribution. The Schur complement $\mathbf{S}$ is a discrete approximation of the Steklov-Poincaré pseudo-differential operator, which in this case maps the interface displacements into the jump in tractions across the interface (see [8] for a discussion in the context of the Poisson equation). Roughly speaking, the condition for convergence (4.11) amounts to the solid contribution to this operator "dominating" the fluid contribution. The inequalities

$$\rho\left(\mathbf{S}_S^{-1}\mathbf{S}_F\right) \leq \sigma_{max}\left(\mathbf{S}_S^{-1}\mathbf{S}_F\right) \leq \|\mathbf{S}_S^{-1}\|_2\,\|\mathbf{S}_F\|_2 = \frac{\sigma_{max}\left(\mathbf{S}_F\right)}{\sigma_{min}\left(\mathbf{S}_S\right)} \tag{4.12}$$

assert that a sufficient condition for convergence is that the largest singular value of $\mathbf{S}_F$ be smaller than the smallest singular value of $\mathbf{S}_S$. As the solid becomes stiffer due to an increase in μ_S and λ_S, the singular values of $\mathbf{S}_S$ increase, while those of $\mathbf{S}_F$ remain unchanged. Therefore, (4.12) implies that if the solid is sufficiently stiff, the iteration will converge. This makes sense: the stiffer the solid, the more reasonable it is to ignore the fluid–interface coupling matrices, i.e. those that reflect the dependence of the flow domain on the interface geometry. Usually, $\sigma_{min}(\mathbf{S}_S) > \sigma_{max}(\mathbf{S}_F)$, since $(\mu_S, \lambda_S) \gg \mu_F$ for typical solids and fluids. However, if the solid structure is near a buckling point, its (geometric) stiffness will be greatly reduced; in fact $\sigma_{min}(\mathbf{S}_S) \to 0$ as a buckling state is approached. In this case, SOM1 may not converge.

4.2. Solution Method II (SOM2): A Newton-Krylov method with domain decomposition preconditioning. As discussed above, one of the difficulties associated with the approximate Newton method SOM1 is that it may not converge, even if the starting point is close to a solution. Convergence is only guaranteed if, asymptotically, the spectral radius of $\mathbf{S}_S^{-1}\mathbf{S}_F$ is smaller than one. Even if the spectral radius is less than one, convergence will occur at a linear rate, and may be very slow, especially if the spectral radius is close to one. These properties of SOM1 motivate the development of a method that will always converge if the starting point is close enough, and that retains the quadratic convergence rate of Newton's method.

This second method uses the preconditioned Generalized Minimum Residual (GMRES) method [22] to solve the linear system (4.3) arising at each Newton step. GMRES is an iterative method for solving the linear system $\mathbf{A}\mathbf{x} = \mathbf{b}$ that, at the i-th step, minimizes the 2-norm of the residual of the linear system, $\mathbf{r}$, over the Krylov subspace

$$\text{span}\{\mathbf{A}^0\mathbf{r}(\mathbf{x}^0), \mathbf{A}^1\mathbf{r}(\mathbf{x}^0), \ldots, \mathbf{A}^{i-1}\mathbf{r}(\mathbf{x}^0)\},$$

in which $\mathbf{A}^i$ indicates the i-th power of $\mathbf{A}$. Because $\mathbf{A}$ is unsymmetric, an orthogonal basis for the Krylov subspace must be found explicitly. The necessary work and storage increase linearly with the iteration count i; thus we use a restarted version, GMRES(m).

Recall that the difficulties associated with solving the Newton equations (4.3) are ill-conditioning of the Jacobian and storage of the potentially large, dense fluid-interface and interface-interface coupling matrices. The use of preconditioned GMRES addresses both of these difficulties. First, we use a preconditioner based on the one-way-coupled approximate Jacobian of SOM1. That is, for the purposes of the preconditioner, we ignore the fluid-interface and interface-interface coupling matrices $\mathbf{J}_{FI}$ and $\mathbf{J}_{II_F}$; the preconditioner is thus $\tilde{\mathbf{J}}$ in (4.9). This allows decomposition into distinct fluid and solid subproblems, similar to the systems (4.6) and (4.7); thus, the preconditioner is easy to apply, especially when a direct method is used to factor the coefficient matrices of (4.6) and (4.7) and the resulting factors are re-applied at each GMRES iteration. The use of this domain decomposition preconditioning has been found to significantly reduce the condition number of the Jacobian matrix, and hence iterations required by GMRES.

The second goal is to avoid the need to compute and store the dense matrices $\mathbf{J}_{FI}$ and $\mathbf{J}_{II_F}$. We have seen that the domain decomposition preconditioner described above meets this criterion. However, the Jacobian matrix, or more precisely its product with some vector $\mathbf{z}$, is required at each GMRES iteration. To avoid computation and storage of $\mathbf{J}_{FI}$ and $\mathbf{J}_{II_F}$, we use the well-known device of recognizing this product as the derivative of $\mathbf{J}$ in the direction of $\mathbf{z}$, and approximate this directional derivative by differencing $\mathbf{h}$ in the direction of $\mathbf{z}$, e.g. the forward difference approximation

$$\mathbf{J}(\mathbf{x}^k)\mathbf{z} \approx \frac{1}{\alpha}\left[\mathbf{h}(\mathbf{x}^k + \alpha\mathbf{z}) - \mathbf{h}(\mathbf{x}^k)\right]. \tag{4.13}$$

Thus, storing $\mathbf{J}_{FI}$ and $\mathbf{J}_{II_F}$ is avoided completely. Note that what prevents SOM2 from being a proper Newton method is the truncation error resulting from a finite difference approximation of the directional derivative, in addition to the residual error in the inner GMRES iteration. The latter can be used to advantage to create a truncated Newton method—the increase in outer (nonlinear) iterations due to loss of formal quadratic convergence is more than compensated for by a reduction in the number of inner (linear) iterations, e.g. [7]. Quadratic convergence may be observed when both truncation and residual error are sufficiently small.

Finally, we remark that both SOM1 and SOM2 are only locally convergent. To globalize, we use a simple continuation scheme on both fluid Reynolds number as well as solid stiffness. Since increasing Reynolds number and decreasing stiffness are associated with a greater degree of nonlinearity, the continuation scheme begins with greater stiffness and lower Reynolds number than those that characterize the given problem. A solution of this problem is obtained, the Reynolds number is increased and the stiffness decreased, and the process is repeated until the target values are reached.

5. Domain decomposition methods for sensitivity analysis of the discrete system. In this section we consider the problem of sensitivity analysis of the coupled nonlinear fluid-solid system. By sensitivity analysis we mean finding derivatives of the solid displacement, and fluid velocity and pressure, fields with respect to some parameter upon which they depend. Derivatives of secondary quantities, such as stress, strain, strain rate, drag, lift, strain energy, and rate of viscous energy dissipation, can be computed from the displacement, velocity, and pressure derivatives.

A distinct advantage of the coupling methodology advanced above is the characterization of the coupled behavior by a single set of nonlinear equations, and hence the ease with which sensitivity analysis can be carried out. Let us consider the problem of finding the sensitivity of the coupled fluid-solid system with respect to some parameter π. Thus the governing state equations (4.1) depend on π both explicitly as well as implicitly through the dependence of the state variables $\mathbf{x}$ on π, i.e.

$$\mathbf{h}\left(\mathbf{x}^*\left(\pi\right), \pi\right) = \mathbf{0}. \tag{5.1}$$

Here, $\mathbf{x}^*$ represents the set of solid, fluid, and interface unknowns that satisfy $\mathbf{h} = \mathbf{0}$ for a given value of π, and $\mathbf{h}$ represents the residual of the fluid-solid system (4.1). Now if we differentiate this system with respect to the parameter π, we obtain the linear system

$$\frac{\partial \mathbf{h}}{\partial \mathbf{x}}\left(\mathbf{x}^*, \pi\right)\frac{d\mathbf{x}}{d\pi} = -\frac{\partial \mathbf{h}}{\partial \pi}\left(\mathbf{x}^*, \pi\right), \tag{5.2}$$

which can be solved for the state variable sensitivity $d\mathbf{x}/d\pi$, once $\mathbf{x}^*$ has been found. We see that sensitivities can be found by solving a linear system of equations with a coefficient matrix that is just the Jacobian of the residual of the state equations with respect to the state variables, evaluated at the converged value of the state variables. Sobieski has termed this the GSE1 approach [23]. Thus, solving the sensitivity equations exploits the same tools developed for Newton-like solution of the state equations, in particular the two domain decomposition methods described above; hence our reason for pursuing this approach over others.

Let us rewrite the sensitivity equations (5.2) as

$$\mathbf{J}\mathbf{x}_\pi = -\mathbf{h}_\pi, \tag{5.3}$$

where the subscript π indicates partial derivative with respect to π, and it is understood that both $\mathbf{J}$ and $\mathbf{h}$ are evaluated at $\mathbf{x}^*$, the solution of the state equations corresponding to the parameter π. The difficulty with solving (5.3) in the context of nonlinear fluid-solid interaction is that it is undesirable to compute, store, and factor the coefficient matrix $\mathbf{J}$, for the same reasons that arose in the design of a solver for the state equations, i.e. density of some of its components as well as its potential ill-conditioning. Below, we introduce two sensitivity analysis methods directly related to the domain decomposition methods for solving the coupled fluid-solid system described in the previous section.

5.1. Sensitivity Method I (SEM1): A stationary iterative method with domain decomposition preconditioning. We consider a stationary iterative method for the sensitivity equations (5.3) that makes use of the splitting

$$\mathbf{J} = \tilde{\mathbf{J}} + \mathbf{J}_c, \tag{5.4}$$

where as before $\tilde{\mathbf{J}}$ is the one-way-coupled block-triangular approximate Jacobian in (4.9), obtained by ignoring the matrices $\mathbf{J}_{FI}$ and $\mathbf{J}_{II_F}$, and $\mathbf{J}_c$ is the defect matrix, i.e. the difference between this approximate Jacobian and the exact one. We can think of $\tilde{\mathbf{J}}$ as the preconditioner. We assume that all quantities are evaluated at $\mathbf{x}^*$.

The iteration induced by this splitting is

$$\tilde{\mathbf{J}}\mathbf{x}_\pi^{k+1} = -\mathbf{J}_c\mathbf{x}_\pi^k - \mathbf{h}_\pi, \tag{5.5}$$

which can be rewritten in the form

$$\begin{aligned} \tilde{\mathbf{J}}\Delta\mathbf{x}_\pi &= -\mathbf{J}\mathbf{x}_\pi^k - \mathbf{h}_\pi, \\ \mathbf{x}_\pi^{k+1} &= \Delta\mathbf{x}_\pi + \mathbf{x}_\pi^k. \end{aligned} \tag{5.6}$$

This last form of the sensitivity equations is equivalent to the incremental iterative method of [19]. The stationary iterative method (5.5) converges (linearly) when

$$\rho\left(\tilde{\mathbf{J}}\left(\mathbf{x}^*\right)^{-1}\mathbf{J}_c\left(\mathbf{x}^*\right)\right) < 1, \tag{5.7}$$

which is identical to the convergence condition (4.8) associated with the one-way-coupled approximate Jacobian method for solving the nonlinear fluid-solid system, i.e. SOM1 above. This intimate relationship between, on one hand, Newton-like approximate Jacobian methods for nonlinear equations, and on the other hand, the use of the same approximate Jacobian splittings in stationary iterative methods for their limiting linear system, is well known, e.g. [20]. Thus the convergence condition is that the spectral radius of $\mathbf{S}_S^{-1}\mathbf{S}_F$ should be less than one. A sufficient condition for convergence is that the solid should be sufficiently stiff. The smaller the spectral radius—the stiffer the solid—the faster the iteration converges.

One difficulty remains in the sensitivity iteration (5.6): the Jacobian matrix $\mathbf{J}$, which we desire not to compute, appears on the right side of the equation, post-multiplied by the vector $\mathbf{x}_\pi^k$. Thus we employ the same device used in SOM2: this matrix-vector product is approximated by differencing the state equations in the direction of the vector, e.g. the forward difference

$$\mathbf{J}\mathbf{x}_{\pi}^{k} \approx \frac{1}{\alpha}\left[\mathbf{h}(\mathbf{x}^{*}+\alpha\mathbf{x}_{\pi}^{k})-\mathbf{h}(\mathbf{x}^{*})\right]. \tag{5.8}$$

Provided $\mathbf{h}_{\pi}$ is computed correctly, the displacement, velocity, and pressure sensitivities thus obtained are exact up to the truncation error of the finite difference approximation of the directional derivative (5.8), in addition to the residual error of the stationary iteration (5.6).

The result is a method for sensitivity analysis that uses a linear solver identical to that used by the one-way-coupled approximate Jacobian method for the nonlinear fluid-solid system. It converges when the associated nonlinear solver converges, and with the same asymptotic rate. The cost of finding sensitivities using this method is very small compared to the cost of solution. This is especially true when direct methods are used to factor the coefficient matrices in (4.6) and (4.7), since these factors (evaluated at the converged point $\mathbf{x}^{*}$) are merely reused at each iteration of the stationary iterative method (5.6).

5.2. Sensitivity Method II (SEM2): A Krylov subspace method with domain decomposition preconditioning. As we have seen, SEM1 is only conditionally convergent—the solid must be stiff enough. Furthermore, Krylov subspace methods are generally more efficient than stationary iterative methods, especially when good preconditioners are available. These two facts motivate the development of a Krylov-based sensitivity method analogous to the Newton-Krylov solver for the nonlinear fluid-solid system.

The linear set of equations (5.3) characterizing sensitivity of the coupled fluid-solid system can be attacked directly by a Krylov method. In fact, since the coefficient matrix of (5.3) is identical to that of the limiting Jacobian of the Newton iteration (4.2), we may use the same GMRES linear solver developed for the nonlinear Newton-Krylov method. Again, we use a domain decomposition preconditioning based on neglecting the two-way coupling, i.e. we use $\tilde{\mathbf{J}}$ in (4.9) as a preconditioner. The only difference between the two linear systems is in the right side: here it is the opposite of the partial derivative of the residual with respect to the parameter π, and not the residual itself. As in the case of SOM2, the directional derivative implied by the matrix-vector product required at each iteration by GMRES is approximated by finite differencing in the direction of the vector. Thus, the matrix $\mathbf{J}$ need never be formed.

The computed sensitivities are again exact, up to the truncation error associated with finite differencing the matrix-vector product, as well as the residual error of the GMRES iteration, provided $\mathbf{h}_{\pi}$ is found exactly. The cost of computing sensitivities using this method is again very cheap relative to the cost of solving using SOM2. Again, this is especially true when direct methods are used for factoring the coefficient matrices in (4.6) and (4.7): the domain-decomposed preconditioner has already been formed in the final Newton step, so re-applying it for sensitivity analysis amounts to two triangular solves at each GMRES iteration.

6. Illustration: viscous flow about an infinite elastic cylinder. In this section we provide an illustration of the computation of sensitivities of the flow of a viscous fluid about an infinite elastic cylinder. The methods used are SOM2 and SEM2. The implementation is for arbitrary two-dimensional geometries. We use Taylor-Hood triangular elements in the fluid, which are quadratic in velocity and linear in pressure, and quadratic triangles in the solid. The displacement and velocity test functions thus agree across the interface, as is required by our formulation. Figure 6.1 shows a portion of a typical triangulation, including a solid portion, a fluid portion, and the interface between the two. The locations of nodal velocity, pressure, and displacement variables are indicated. The Taylor-Hood element is known to satisfy

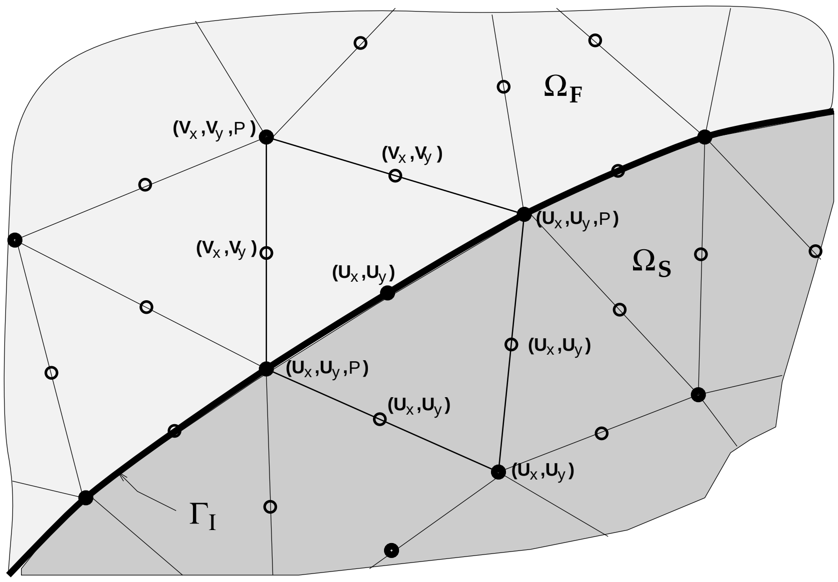

FIG. 6.1. *Interface between solid and fluid, showing typical triangulation and location of unknowns. Vertex nodes include both velocity and pressure variables in the fluid, and displacement variables in the solid. Mid-side nodes represent just velocity unknowns in the fluid, and displacement unknowns in the solid. The interface variables do not include velocities, due to the no-slip condition.*

the LBB stability condition [12]. Since the implementation is 2D, we use a direct solver, namely the sparse LU factorization code UMFPACK [9], to perform the linear solves (4.6) and (4.7) that are common to all four methods. The righthand side of (5.2) is found analytically. Simple continuation on Reynolds number and solid stiffness is used to globalize the Newton solver.

As the solid deforms, so does the surrounding fluid. Since we have assumed that solid strains remain small, there is no need to remesh the solid domain. However, large displacements on the interface necessitate remeshing of the deforming fluid domain. This is carried out by treating the fluid as an elastic continuum, discretized by the same triangulation used to approximate the Navier-Stokes equations; this idea dates to at least [5]. Interface deformation is then effected as an inhomogeneous Dirichlet boundary condition for the elasticity equations, i.e. by imposed displacements. Solving the elasticity equations over the fluid domain (by finite elements) yields a displacement field that is added to the current coordinates of the mesh, yielding a deformed mesh. The advantages of this approach include its smoothness (mesh coordinates depend smoothly on interface motion), and that it requires little beyond the existing tools for solving the fluid-solid interaction problem.

We consider the problem of viscous flow about an infinite, elastic cylinder. The geometry and properties are depicted in Figure 6.2. Flow is from left to right; the cylinder is fixed at the downstream side, along the axis of symmetry of the problem. The upstream side of the cylinder is prevented from translating normal to the axis

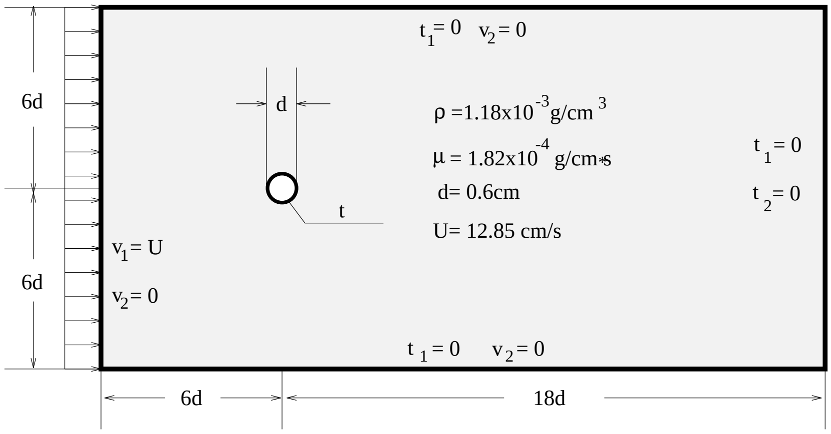

FIG. 6.2. *Elastic cylinder surrounded by viscous, incompressible fluid.*

of symmetry. The outflow boundary condition consists of zero transverse and normal traction. The Reynolds number of the flow—50—is kept low to insure a stationary solution. The Poisson ratio of the solid is taken to be 0.3. A typical mesh is shown in Figure 6.3. Mesh data are provided in Table 6.1. The scale of the figures is too small

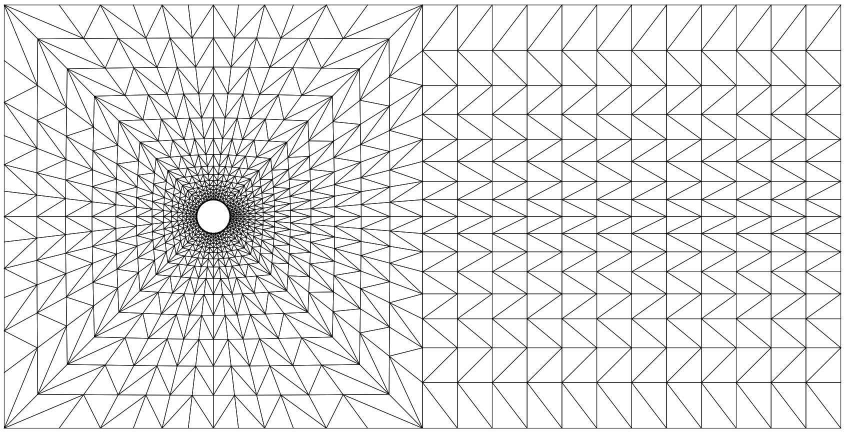

FIG. 6.3. *Finite element mesh.*

to show the discretization of the cylinder; in fact we use two elements (and thus five nodes) through its thickness. The mesh is of course conforming across the interface, as required by our formulation. A single tolerance of 10^{-6} in the L_2 norm is used to define convergence of the outer nonlinear iteration for SOM2, the GMRES iteration for SOM2 and SEM2, and the step size for the forward difference approximation of the directional derivative in SEM2. The number of vectors stored by GMRES, m, is fixed at 20.

Figure 6.4 shows a portion of the flowfield in the vicinity of the cylinder corresponding to a nearly rigid cylinder (elastic modulus of 10,000; cylinder thickness of 0.06). The deformation of the cylinder is undetectable. Streamlines about a more flexible cylinder (elastic modulus of 1000, thickness of 0.02) are displayed in Figure 6.5. The cylinder is seen to undergo a large deformation, and the standing eddies just

TABLE 6.1
Mesh data

item	number
solid nodes	416
fluid nodes	3552
interface nodes	104
boundary nodes	152
total nodes	4224
solid elements	208
fluid elements	1840
total elements	2048
velocity unknowns	7166
pressure unknowns	984
displacement unknowns	824
interface unknowns	205
total unknowns	9179

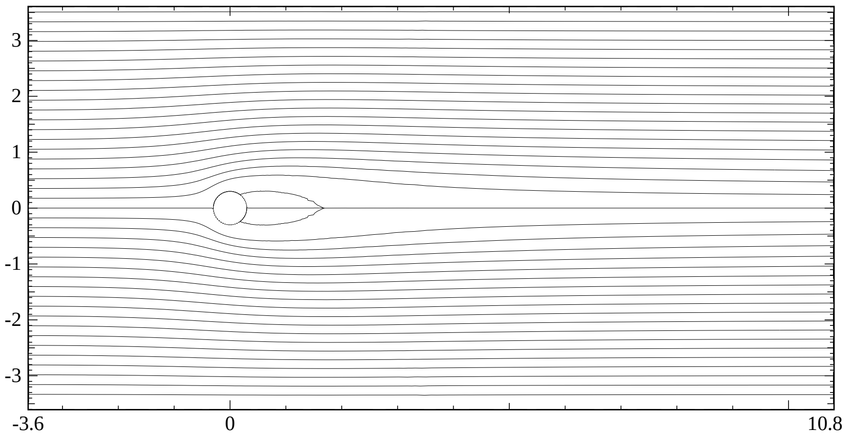

FIG. 6.4. *Viscous flow about stiff cylinder.*

behind the cylinder extend much further downstream due to its more bluff shape.

Figures 6.6 and 6.7 show displacement and velocity sensitivity fields. The velocity and displacement sensitivities, since they represent derivatives of vector fields with respect to a scalar quantity, are displayed as vector fields—direction and magnitude are indicated by the direction and length of the arrows. In addition, displacement sensitivities are shown only at interface nodes for clarity. Figure 6.6 presents the sensitivity of field quantities with respect to the elastic modulus of the solid, for the case of the stiff cylinder (the flow around which was shown in Figure 6.4). The displacement field sensitivity is seen to be zero at the support and symmetric about the centerline, as expected. It is greatest at the upstream side of the cylinder, which is anticipated since for the given direction of the flow, the largest displacements occur here, so any increase in stiffness yields a greater reduction in displacement than at other points. Finally, the displacement field sensitivity points in the direction of an ellipse, with major axis aligned with the flow. Again this makes sense since the

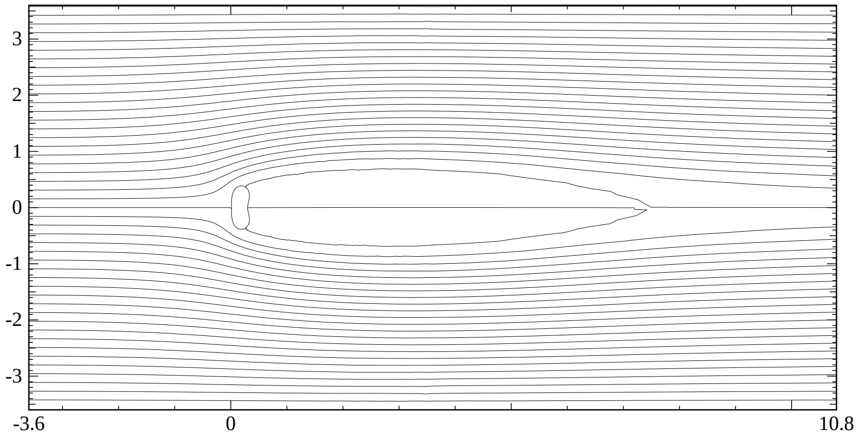

FIG. 6.5. *Viscous flow about soft cylinder.*

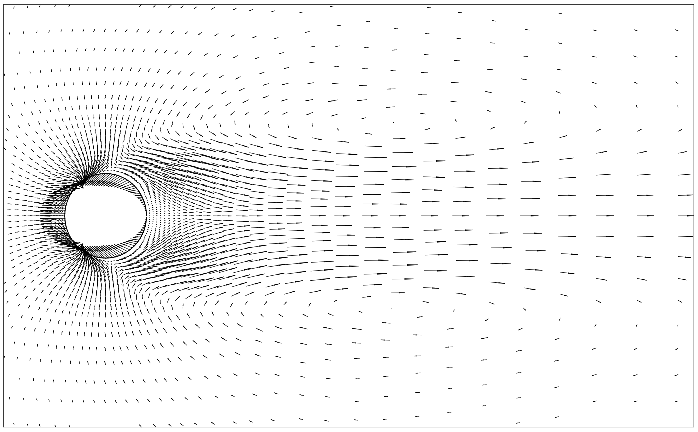

FIG. 6.6. *Sensitivity of velocity and displacement fields to elastic modulus for a stiff cylinder.*

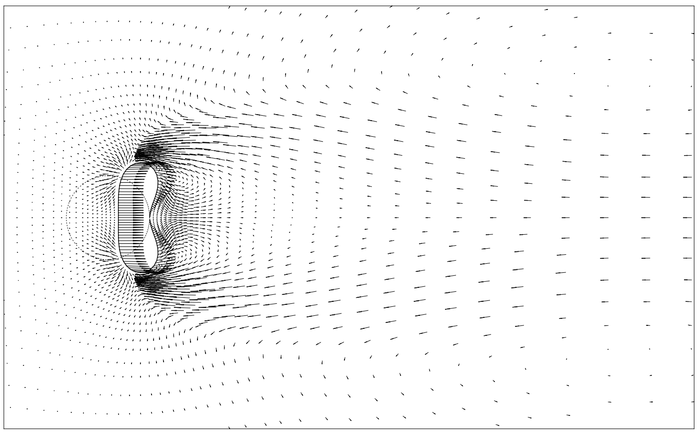

FIG. 6.7. *Sensitivity of velocity and displacement fields to viscosity for a soft cylinder.*

deformed shape (too small to be seen, but expected given this flow scenario) is elliptical but with major axis aligned transverse to the flow. So the change in displacement due to an increase in elastic modulus (i.e. the sensitivity) is moving towards restoring the circular shape, which is the deformed shape we obtain in the limit as the cylinder becomes perfectly rigid.

The sensitivity of the fluid velocity field to elastic modulus shown in Figure 6.6 is also consistent with what we intuitively expect. The sensitivity tends to zero as one approaches the cylinder surface, since the no-slip boundary condition is always maintained regardless of the elastic modulus. Upstream of the cylinder, we expect the velocity sensitivity to be minimal, and it is. The sensitivity is greatest in the wake region, downstream of the cylinder. For the stiff cylinder, an increase in stiffness creates a a more circular and less-blunt deformed shape, which reduces the length of the standing eddies behind the cylinder, resulting in an increase in velocity in this region—hence the positive velocity sensitivities in the wake of the cylinder. Of course, in the absence of fluid–solid interaction, the velocity sensitivity would be zero.

Sensitivities of velocity and displacement fields to fluid viscosity, for the soft cylinder, are shown in Figure 6.7. The flowfield for this problem was shown in Figure 6.5. The sensitivity of the solid displacement field at interface nodes on the cylinder surface is shown in the figure. As viscosity increases, fluid tractions acting on the solid surface increase, which leads to greater deformation of the cylinder cross-section, as indicated by the magnitude and direction of the sensitivity vectors. The direction is towards an even more crushed shape, as expected for this flow scenario. Again the displacement sensitivities are symmetric about the centerline of the cylinder, and the support point on the downstream side of the cylinder has a zero displacement sensitivity, since the boundary condition there is independent of the viscosity. An increase in viscosity causes a reduction in Reynolds number, which should reduce the length of the standing eddies behind the cylinder. On the other hand, a greater viscosity creates a more blunt deformed cylinder as argued above, and this effect would lead to an increase in length of the standing eddies in the wake. The two effects thus tend to counteract each other, and the resulting fluid velocity sensitivities in the wake region are much smaller than those in Figure 6.6.

In both examples presented above, we have compared sensitivities obtained from SEM2 with those of central difference approximations; the results are visually indistinguishable from each other. We have also implemented SOM1 and SEM1, and comparisons with the sensitivities obtained with that approach are also indistinguishable. A comparison between the performance of the SOM1/SEM1 and SOM2/SEM2 approaches will be forthcoming.

We are currently working on extending the variational finite element method, coupled fluid-solid solver, and sensitivity algorithms described in this paper to unsteady nonlinear fluid-solid interaction in three dimensions. Our ultimate goal is design optimization of coupled solid-fluid systems, a task for which the analysis and sensitivity methods presented here are well-suited, as a result of their expressing system behavior and sensitivity each as a single set of equations.

REFERENCES

[1] AIAA, *Fourth AIAA/USAF/NASA/OAI Symposium on Multidisciplinary Analysis and Optimization*, Cleveland, OH, September 1992.

[2] ———, *Fifth AIAA/NASA/USAF/ISSMO Symposium on Multidisciplinary Analysis and Optimization*, Panama City, FL, September 1994.

[3] ———, *Sixth AIAA/NASA/ISSMO Symposium on Multidisciplinary Analysis and Optimization*, Bellevue, WA, September 1996.

[4] N. M. Alexandrov and M. Hussaini, eds., *Multidisciplinary Design Optimization: State-of-the-Art*, SIAM, 1997.

[5] J. Argyris, J. Doltsinis, H. Fischer, and H. Wüstenberg, $T\alpha\ \pi\alpha\nu\tau\alpha\ \rho\varepsilon\iota$, Computer Methods in Applied Mechanics and Engineering, 51 (1985), pp. 289–362.

[6] J. Arora, *Design sensitivity analysis of nonlinear structures*, in Multidisciplinary Design Optimization: State-of-the-Art, N. M. Alexandrov and M. Hussaini, eds., SIAM, 1997, pp. 243–262.

[7] P. Brown and Y. Saad, *Hybrid Krylov methods for nonlinear systems of equations*, SIAM Journal on Scientific and Statistical Computing, 11 (1990), pp. 450–481.

[8] T. F. Chan and T. P. Mathew, *Domain decomposition algorithms*, in Acta Numerica 1994, Cambridge University Press, 1994, pp. 61–144.

[9] T. A. Davis and I. S. Duff, *An unsymmetric pattern multifrontal method for sparse LU factorization*, Tech. Rep. TR-93-018, CIS Dept., Univ. of Florida, Gainesville, FL, 1993.

[10] C. Farhat, M. Lesoinne, and N. Maman, *Mixed explicit/implicit time integration of coupled aeroelastic problems: Three-field formulation, geometric conservation and distributed solution*, International Journal for Numerical Methods in Engineering, 21 (1995), pp. 807–835.

[11] O. Ghattas and X. Li, *A variational finite element method for stationary nonlinear fluid-solid interaction*, Journal of Computational Physics, 121 (1995), pp. 347–356.

[12] M. D. Gunzburger, *Finite Element Methods for Viscous Incompressible Flows*, Academic Press, 1989.

[13] M. D. Gunzburger, L. S. Hou, and T. P. Svobodny, *Optimal control and optimization of viscous, incompressible flows*, in Incompressible Computational Fluid Dynamics, M. D. Gunzburger and R. A. Nicolaides, eds., Cambridge, 1993, ch. 5, pp. 109–150.

[14] G. Guruswamy, *Unsteady aerodynamic and aeroelastic calculations for wings using the Euler equations*, AIAA Journal, 28 (1990), pp. 461–469.

[15] ———, *Vortical flow computations on swept flexible wings using Navier-Stokes equations*, AIAA Journal, 28 (1990), pp. 2077–2084.

[16] ———, *Vortical flow computations on a flexible blended wing-body configuration*, in 32nd Structures, Structural Dynamics, and Materials Conference, AIAA, 1991, pp. 719–734.

[17] ———, *Coupled finite-difference/finite element approach for wing-body aeroelasticity*, in Fourth AIAA/USAF/NASA/OAI Symposium on Multidisciplinary Analysis and Optimization, 1992, pp. 1–12.

[18] R. Haftka and Z. Gürdal, *Elements of Structural Optimization*, Kluwer Academic, third ed., 1991.

[19] V. Korivi, A. Taylor, P. Newman, G. Hou, and H. Jones, *An approximately factored incremental strategy for calculating consistent discrete aerodynamic sensitivity derivatives*, in Proceedings of the Fourth AIAA/USAF/NASA/OAI Symposium on Multidisciplinary Analysis and Optimization, AIAA, 1992, pp. 465–478.

[20] J. Ortega and W. Rheinboldt, *Iterative Solution of Nonlinear Equations in Several Variables*, Academic Press, 1970.

[21] S. Piperno, C. Farhat, and B. Larrouturou, *Partitioned procedures for the transient solution of coupled aeroelastic problems*, Computer Methods in Applied Mechanics and Engineering, 124 (1995), pp. 79–112.

[22] Y. Saad and M. Schultz, *GMRES: A generalized minimal residual algorithm for solving nonsymmetric linear systems*, SIAM Journal on Scientific and Statistical Computing, 7 (1986), pp. 856–869.

[23] J. Sobieszczanski-Sobieski, *Sensitivity of complex, internally coupled systems*, AIAA Journal, 28 (1990), pp. 153–160.